

A Novel Thiol-Modified Hyaluronan and Elastin-Like Polypeptide Composite Material for Tissue Engineering of the Nucleus Pulposus of the Intervertebral Disc

Isaac L. Moss, MDCM, MASC,*† Lyle Gordon, BSc,† Kimberly A. Woodhouse, PhD,†‡ Cari M. Whyne, PhD,*† and Albert J.M. Yee, MD, MSc,*†

Study Design. Biomechanical, *in vitro*, and initial *in vivo* evaluation of a thiol-modified hyaluronan (TM-HA) and elastin-like polypeptide (ELP) composite hydrogel for nucleus pulposus (NP) tissue engineering.

Objective. To investigate the utility of a TM-HA and ELP composite material as a potential tissue-engineering scaffold to reconstitute the NP in early degenerative disc disease (DDD) on the basis of both biomechanical and biologic parameters.

Summary of Background Data. DDD is a common ailment with enormous medical, psychosocial, and economic ramifications. Only end-stage surgical therapies are currently widely available. A less invasive, early stage therapy may provide a clinically relevant treatment option.

Methods. TM-HA and ELP were combined in various concentrations and cross-linked using poly (ethylene glycol) diacrylate. Resulting materials were evaluated biomechanically using confined compression to determine biphasic material properties. *In vitro* cell culture with human intervertebral disc (IVD) cells seeded within TM-HA/ELP scaffolds was analyzed for cell viability and phenotype. The hydrogels' materials were evaluated in an established New Zealand White (NZW) rabbit model of DDD.

Results. The addition of ELP to TM-HA-based hydrogels resulted in a stiffer construct, which is less stiff than native NP but has time-dependant loading characteristics that may be desirable when

injected into the IVD. *In vitro* experiments demonstrated 70% cell viability at 3 weeks with apparent maintenance of phenotype on the basis of morphologic and immunohistochemical data. The addition of ELP had a positive desirable biomechanical effect but did not have a significant positive or negative biologic effect on cell activity. The *in vivo* feasibility study demonstrated favorable material characteristics and biocompatibility for application as a minimally invasive injectable NP supplement.

Conclusions. TM-HA-based hydrogels provide a hospitable environment for human IVD cells and have material characteristics, particularly when supplemented with ELPs that are attractive for potential application as an injectable NP supplement.

Key words: intervertebral disc, elastin, hyaluronan, hydrogel, tissue engineering, biomechanics. **Spine 2011;36:1022–1029**

There are limited treatment options available for patients with symptomatic intervertebral disc (IVD) degeneration. Current surgical management of degenerative disc disease (DDD) is primarily directed toward end-stage disease; however, there has been considerable enthusiasm in tissue-engineered and cell-based strategies that hold future promise in treating early disease. In early degeneration, damage is predominantly in the nucleus pulposus (NP) of the IVD, resulting in loss of aggrecan and key extracellular matrix (ECM) components.¹ The glycosaminoglycan hyaluronan (HA) is considered an essential ECM component of the IVD and forms large proteoglycan aggregates through interaction with aggrecan, link protein, and other ECM molecules. These interactions are mechanically important for the load-bearing function of NP tissue and the IVD.

HA has been explored as a possible treatment of IVD degeneration. Stern *et al*² observed that porcine NP cells cultured in fibrin/HA matrix expressed higher levels of proteoglycans when compared with alginate cell cultures. Injection of high-molecular weight HA into a primate DDD model demonstrated improved gross, histologic, and radiographic outcomes.³ Several other investigators have observed HA-based scaffolds to be a hospitable environment for NP cells.^{4–8} Despite these positive observations, formulations of HA commercially available, and those previously investigated behave as viscous liquids and material extravasation from the IVD

From the *Department of Surgery, University of Toronto, Toronto, Ontario, Canada; †Advanced Regenerative Tissue Engineering Centre (ARTEC)/Orthopaedics Biomechanics Laboratory (OBL), Sunnybrook Research Institute, Sunnybrook Health Sciences Centre, Toronto, Ontario, Canada; and ‡Faculty of Applied Science, Queen's University, Kingston, Ontario, Canada.

Acknowledgment date: March 9, 2010. Revision date: April 27, 2010. Acceptance date: May 10, 2010.

The manuscript submitted does not contain information about medical device(s)/drug(s).

Funding for this work was provided by the Ontario Centres of Excellence and Elastin Specialties.

One or more of the author(s) has/have received or will receive benefits for personal or professional use from a commercial party related directly or indirectly to the subject of this manuscript.

Address correspondence and reprint requests to Albert J.M. Yee, MD, Sunnybrook Health Sciences Centre, 2075 Bayview Ave, Room MG371B, Toronto, Ontario, Canada; E-mail: Albert.Yee@sunnybrook.ca

DOI: 10.1097/BRS.0b013e3181e7b705

postinjection can occur. Enhancing material containment after therapeutic delivery in addition to improving biomechanical material properties to withstand physiologic loading may improve therapeutic effect. Recent advances include a thiol-modified hyaluronan (TM-HA) that has been synthesized with the ability to form cross-linked hydrogels.⁹ Although TM-HA possesses desirable gelling conditions with short cross-linking time using poly (ethylene glycol) diacrylate (PEGDA), the addition of fibers to cross-linked hydrogels may further enhance structural integrity. Elastin is another ECM molecule found in tissues requiring elastic recoil and is attractive considering the spinal motion segment's dynamic *in vivo* activity. We have explored fiber reinforcement of TM-HA hydrogels using a purified family of elastin-like polypeptides (ELPs), which has been synthesized to exhibit properties similar to natural human elastin.¹⁰ Thus, this study was designed to investigate the hypothesis that the addition of ELPs to TM-HA would enhance the biologic and mechanical properties of tissue-engineered NP constructs in degenerative IVD therapy.

MATERIALS AND METHODS

Study Outline

TM-HA and ELP were combined in various concentrations and cross-linked using PEGDA. Resulting materials were evaluated biomechanically by confined compression testing. *In vitro* cell culture with human IVD cells seeded within TM-HA/ELP scaffolds were analyzed for cell viability and phenotype. The hydrogels' materials were evaluated in an established New Zealand White (NZW) rabbit model of DDD.

Scaffold Materials

TM-HA was provided by Dr. G Prestwich (Salt Lake City, UT) and was synthesized as described by Shu *et al.*⁹ In this study, the investigators used PEGDA (MW 3400 Da, Layсан Bio, Arab, AL) to shorten the cross-linking time to approximately 10 minutes. EP4, the ELP used in this study (Elastin Specialties, Toronto, ON), was synthesized in transformed *E. coli* using lab-scale fermentation.¹¹ EP4 is composed of five hydrophobic domains (exon 20 or 24) flanking four cross-linking domains (exon 21 and 23). EP4 peptides have been shown to coacervate and possess material properties similar to native elastin.¹⁰

IVD Cell-Scaffold Evaluation

After appropriate institutional review board approval, fresh human IVD specimens, composed of NP tissue, were harvest-

ed from patients undergoing spinal surgery for disc herniation and/or spinal stenosis with instability. Morselized IVD tissue was subject to sequential enzymatic digestion as described by Chiba *et al.*¹² The digested tissue was filtered; isolated IVD cells were suspended in low-glucose Dulbecco's Modified Eagle's Medium (DMEM, Sigma, St Louis, MO) containing 1% P/S and with 10% Fetal Bovine Serum (FBS, Wisent Inc., Rouville, QC) and cultured in monolayer. Culture media was changed three times per week, and cells were passaged as necessary, not exceeding four passages.¹³ When the isolated cells were sufficiently expanded, cultured cells were trypsinized and suspended in serum-free DMEM containing 1% P/S at a cell density of 10^6 cells/50 μ L.

Solutions of TM-HA alone and a 3:1 TM-HA:EP4 formulation were combined with the cell suspension (10^6 cells/sample) at a final TM-HA concentration of 1.5% (Table 1). The cell expansion from each individual patient was divided and seeded into both scaffold formulations to account for intersample variability. In one case from each formulation, a seeded scaffold was discarded because of contamination; thus, three of four samples from each formulation were seeded by cells from the same patients. For control scaffolds, 50 μ L of DMEM was substituted for the cell suspension to ensure that there was no significant nonspecific scaffold staining using the methods in this study.

TM-HA/cell or TM-HA/EP4/cell suspensions (320 μ L) were combined with 80 μ L of 4% PEGDA in a 48-well plate and incubated (20 minutes). Gelled scaffolds were removed from their molds and placed in 12-well tissue culture plates. Constructs were incubated at 37°C in 5% CO₂ and fed with 3 mL of DMEM (containing 10% FBS, 1% P/S containing 50 μ g/mL, and vitamin C [Sigma, St. Louis, MO]) three times per week. For each time point (1 week and 3 weeks), two TM-HA, two 3:1 TM-HA/EP4 cell-scaffold constructs, and one cell-free control scaffold of each formulation were prepared.

Cell viability was assessed by Live/Dead (Molecular Probes, Carlsbad, CA) fluorescent staining. Laser scanning confocal microscopy was used to visualize the scaffolds and cells in 40 representative images spaced 5 μ m apart throughout the depth of each scaffold (Carl Zeiss LSM510, Thornwood, NY). Of these, eight equally spaced images were analyzed using ImageJ software (Freeware, NIH, Bethesda, MD), quantifying the overall number of cells/image and the percentage of live/dead cells per image. The mean number of cells and percent viable cells were calculated for each scaffold. Means were compared using repeated measures ANOVA in SPSS

TABLE 1. Composition of Hydrogel Scaffolds for *In Vitro* Experiments

	TM-HA only	TM-HA Control	TM-HA/EP4 3:1	3:1 Control
TM-HA (Vol, conc.)	270 μ L, 1.8%	270 μ L, 1.8%	230 μ L, 2.1%	230 μ L, 2.1%
EP4 (4% w/v)	—	—	40 μ L	40 μ L
Cell Suspension (10^6 cells/50 μ L)	50 μ L	—	50 μ L	—
Serum-free DMEM	—	50 μ L	—	50 μ L
PEGDA (4% w/v)	80 μ L	80 μ L	80 μ L	80 μ L

15 (Chicago, IL). Tukey's Honestly Significant Difference was used for *post hoc* comparison.

Immunohistochemistry was performed after 3 weeks of culture. Cell-scaffolds constructs were fixed with 4% paraformaldehyde (Sigma) and washed with blocking solution consisting of Hank's Balanced Salt Solution (Wisent Inc., Rouville, QC), 4% bovine serum albumin (Sigma), and 2% goat serum (Jackson ImmunoResearch, West Grove, PA). Cells were permeabilized with 0.1% Triton-X (Fisher Scientific, Ottawa, ON) and then left to incubate in blocking solution overnight at 4°C. Samples were incubated with rabbit anti-human collagen type II polyclonal antibody (Abcam, Cambridge, MA) and fluorescently labeled with an fluorescein isothiocyanate conjugated donkey antirabbit secondary antibody (Jackson ImmunoResearch, West Grove, PA). Nuclei were counterstained with 7-amino-actinomycin D (7AAD, Sigma). Controls were stained with only secondary antibodies and nuclear stain. The stained scaffolds were imaged using confocal microscopy.

Biomechanical Characterization

Hydrogel scaffolds were created using TM-HA solutions of 1.5%, 1.71%, 1.85%, and 2.4% (w/v) prepared by dissolving lyophilized TM-HA in DMEM at 37°C for 45 minutes. Sodium hydroxide solution was added to adjust the pH to 7.4. lyophilized EP4 was dissolved in DMEM (concentration = 40 mg/mL). The EP4 solution was sterile filtered on ice and then allowed to coacervate by incubating at 37°C. A 4% PEGDA solution in phosphate buffered saline was prepared for cross-linking.

We evaluated TM-HA alone and TM-HA:EP in a 3:1 ratio on a by-weight basis, with final concentration of TM-HA at 1.5% w/v. Additional constructs were tested mechanically with higher proportions of elastin (TM-HA:EP at 1:1 and 2:1 ratios). pH was adjusted to 7.4 with NaOH before cross-linking. The 4% PEGDA solution was then added in a 4:1 (TM-HA:EP:PEGDA) by volume ratio. Two hundred μ L of HA/EP/PEGDA mixture was pipetted into a 6.85-mm diameter polytetrafluoroethylene confinement chamber and incubated at 37°C for 20 minutes until complete material gellation.

Confined compression testing was conducted on the hydrogels at 37°C within a custom-made chamber attached to a micromechanical testing system (800LE, TestResources, Shakopee, MN). After initial equilibration, each specimen was subjected to four successive stress-relaxation cycles with displacements corresponding to 10%, 20%, 30%, and 40% compressive strain (displacement rate 0.5 μ m/s). After each successive strain level, the specimens were allowed the time to relax to equilibrium. Mean peak stresses were recorded at each strain level tested. Data were curve fit to the nonlinear finite deformation biphasic model of Holmes and Mow¹⁴ that describes viscoelastic behavior using four material parameters: H_{A0} , *aggregate modulus* at zero strain, representing the slope of the stress-strain curve at equilibrium; β , the *compressive-stiffening coefficient*, describing how stress changes with increasing strains; k_0 , the *hydraulic permeability* of the tissue in the unloaded state; and M , the *nonlinear permeability coef-*

ficient, describing the change in permeability with increasing strain. As formulated by Perie *et al.*,¹⁵ the pertinent equations, when simplified for one dimension are as follows:

$$\sigma^e = \frac{1}{2} H_{A0} \left(\frac{\lambda^2 - 1}{\lambda^{2\beta+1}} \right) e^{[\beta(\lambda^2 - 1)]} \quad (1)$$

Where σ^e is elastic stress, and λ is solid matrix stretch. The permeability relationship is described as:

$$k = k_0 \left(\frac{\lambda - \Phi_0^s}{1 - \Phi_0^s} \right)^2 e^{[M(\lambda^2 - 1)/2]} \quad (2)$$

where Φ_0^s is the initial solid content. Equations (1) and (2) are related through the following one-dimensional nonlinear partial differential equation:

$$\frac{\delta \sigma^e}{\delta \lambda} \frac{\delta^2 u}{\delta z^2} = \frac{\lambda}{k} \frac{\delta u}{\delta t} \quad (3)$$

where u is defined as the axial deformation, z is the axial coordinate, and t is time.

Scaffold Evaluation in Preclinical Animal Model

After institutional animal care committee approval, an NZW rabbit annular puncture model of IVD degeneration¹⁶ was used for *in vivo* hydrogel evaluation. TM-HA, EP4, and PEGDA solutions were prepared as described earlier using sterile phosphate buffered saline to generate TM-HA only and 3:1 TMHA:EP4 hydrogels without the addition of cells. Eight ($n = 4$ TM-HA, $n = 4$ TM-HA/EP4) skeletally mature rabbits (3.5–4.5 kg) were anesthetized and underwent a left ventrolateral approach to access their lumbar spines. Three lumbar discs in each animal were punctured to a depth of approximately 5 mm with an 18-gauge needle. One randomly selected disc was treated with 100 μ L of TM-HA/PEGDA, a second disc was treated with TMHA/EP4/PEGDA, and the remaining untreated punctured disc served as a control. Fluoroscopic imaging intraoperatively confirmed treated spinal levels. Animals were recovered from anesthesia, provided perioperative antibiotics and analgesia, and permitted ad lib cage activity.

Before the surgery and at 6 and 12 weeks after surgery, anesthetized rabbits underwent T2-weighted fast spin echo magnetic resonance imaging (MRI; 3T Signa General Electric imaging system, Piscataway, NJ). Sagittal plane DICOM images were loaded into Amira 3.1 (Visage Imaging, Carlsbad, CA) for analysis. Disc volume and mean signal intensity were calculated on the basis of image segmentations. Each disc was evaluated on three separate occasions and the resulting volumes and intensities averaged. An "MRI index" was calculated by multiplying the IVD volume with the mean signal intensity in a manner similar to that described by Sobajima *et al.*¹⁷ The data from each disc at 6 and 12 weeks were normalized to the corresponding preoperative data and expressed as a percentage of preoperative values. Mean, volume, and MRI indexes were compared using repeated measures ANOVA in SPSS 15. Tukey's Honestly Significant Difference was used for *post hoc* comparison.

After the 12-week MRI, animals were killed. The lumbar spines were harvested and fixed in 10% neutral buffered

formalin. Experimental and control spinal motion segments were isolated, decalcified (10% formic acid solution [Sigma]), and embedded in paraffin. Tissue samples were stained with hematoxylin & eosin (H&E) and alcian blue. Slides were examined in a blinded fashion and discs graded for degeneration severity.¹⁶

RESULTS

Disc Cell-Scaffold Results

Disc samples from five human subjects (aged 30–65 years) were harvested, expanded, and seeded into 4 TM-HA and 4 TM-HA/EP4 scaffolds and imaged after 1 or 3 weeks of culture. Confocal imaging revealed an even distribution of cells within the scaffolds (Figure 1). IVD cells, which had taken on a spindle-like appearance while in monolayer culture, demonstrated the spherical morphology typical of IVD cells. Means of 118 ± 21 and 104 ± 29 cells per image were found at 1 week in TM-HA and TM-HA/EP4 scaffolds, respectively. This decreased significantly ($P = 0.035$) to a mean of 96 ± 30 and 83 ± 37 cells per image in respective constructs at 3 weeks. Viability analysis revealed a significant decrease ($P = 0.001$) from $77\% \pm 2\%$ and $79\% \pm 4\%$ viable cells at 1 week to $69\% \pm 5\%$ and $70\% \pm 5\%$ viable cells at 3 weeks in TM-HA and TM-HA/EP4 scaffolds, respectively. There was no significant difference in these measures comparing the two scaffold types ($P = 0.961$ for cells/image; $P = 0.828$ for viability). Collagen type II immunohistochemical staining was observed in cell-seeded TM-HA and TM-HA/EP4. Staining was most intense in the pericellular region (Figure 2A, B). There was a minimal amount of nonspecific staining in control hydrogels.

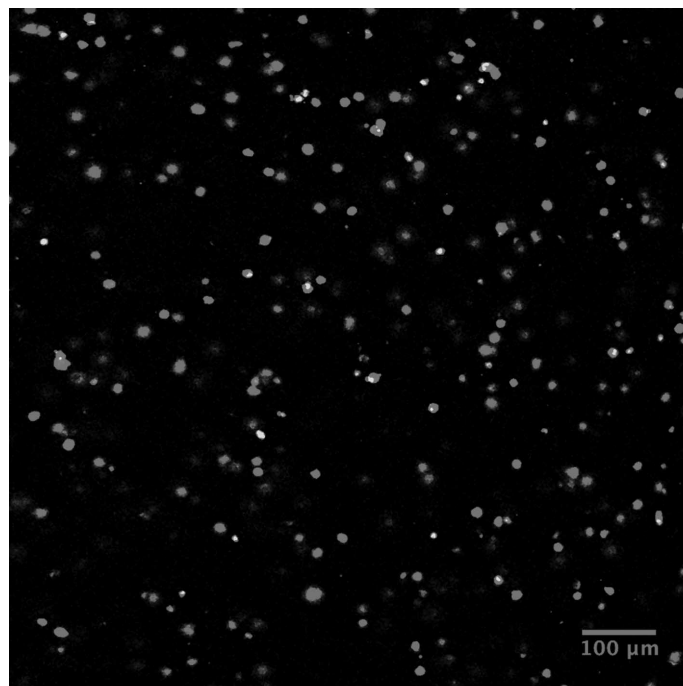
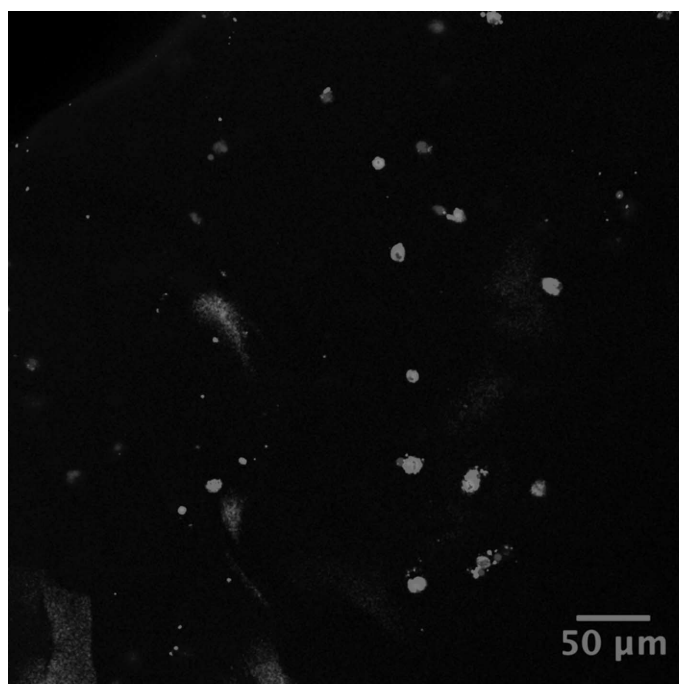


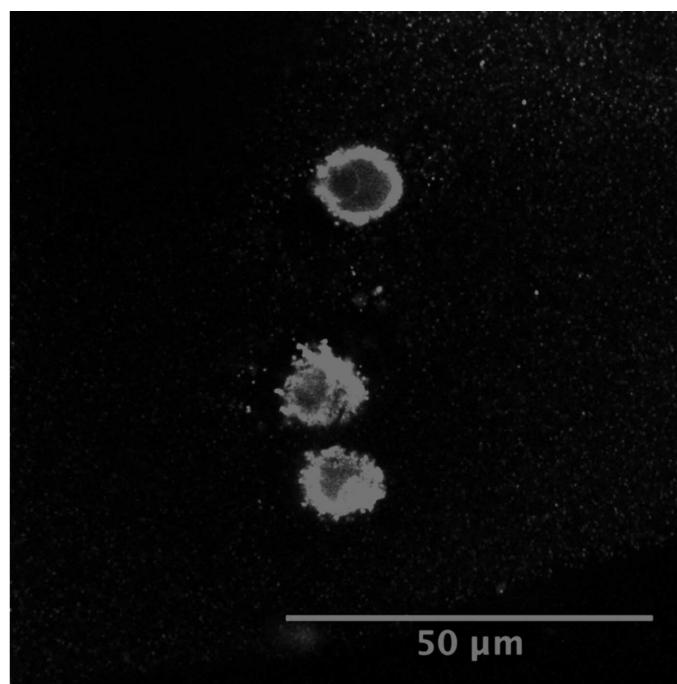
Figure 1. Representative confocal microscope image of live/dead staining of human intervertebral disc cells 3 week after seeding onto a TM-HA/ELP4 scaffold. Live cells fluoresce green, nuclei of dead cells fluoresce red.

Biomechanical Testing

Mean H_{A0} and β were determined for all formulations with good fit of the equilibrium stress-strain data to the model (mean $R^2 = 0.93$; Table 2). Addition of EP4 in a 3:1 or 1:1 ratio to TM-HA resulted in a statistically significant increase in H_{A0} ($P = 0.007$ and $P < 0.001$, respectively). As described earlier, curve fitting



(A)



(B)

Figure 2. Immunohistochemistry for collagen type II. Confocal microscope images of IVD cells seeded into TM-HA/EP4 scaffold after 3 weeks of culture at 20× (A) and 100× (B) magnification demonstrating pericellular expression of type II collagen (green staining).

TABLE 2. Mean Initial Aggregate Modulus (H_{A0}) and Compressive Stiffening Coefficient (β) for Hydrogel Formulations Tested

Formulation	H_{A0}	β
TM-HA	17.0 ± 4.8 KPa*	0
3:1	27.4 ± 3.3 KPa*	0
2:1	23.8 ± 6.1 KPa	0.11
1:1	31.4 ± 4.8 KPa*	0

*Statistically significant differences ($P < 0.05$) as compared with the TM-HA only formulation.

confined compression data to the nonlinear biphasic model of Holmes and Mow¹⁴ yields four material parameters (H_{A0} , β , k_0 , and M). However, acceptable curve fits could not be resolved for both the confined compression stress peaks and equilibrium stresses. If material permeability parameters (*i.e.*, k and M) were adjusted to fit the confined compression stress peaks, the biphasic model predicted equilibrium stresses much higher than those attained experimentally (Figure 3A). Conversely, if material parameters were adjusted to fit the equilibrium stresses, the model predicted peaks significantly lower than those attained experimentally (Figure 3B). No significant differences were found in peak stress between any formulations at 10% or 20% strain (Table 3). The 1:1 formulation was found to have significantly higher peak stress than the TM-HA only at 30% and 40% compressive strain ($P = 0.007$ – 0.013) and the 3:1 ratio at 30% strain only ($P = 0.009$).

In Vivo Animal Results

The mean volume, signal intensity, and MRI index (volume \times signal intensity) in all punctured discs (hydrogel treated

and untreated) decreased significantly throughout the experimental period when compared with nonpunctured normal discs. The average decline in disc volume and signal intensity was lower in the TM-HA and TM-HA/EP4-treated discs compared with controls (Figure 4); however, this did not reach statistical significance given data variance and sample size evaluated in this feasibility experiment. A similar trend was observed toward a better maintenance of histologic IVD grade in both TM-HA (mean Grade 6.9/12) and TM-HA/EP4 (mean Grade 8.9/12) treated IVDs when compared with injured but untreated IVDs (mean Grade 10.3/12). TM-HA and TM-HA/EP4 was observed in histologic sections through 12 weeks. No significant inflammatory reaction was demonstrated in the treated IVDs. Alcian blue staining was qualitatively more intense in treated discs from both hydrogel groups, suggesting a higher proteoglycan content when compared with punctured but untreated discs (Figure 5).

DISCUSSION

This study reports, to our knowledge, the first investigation of TM-HA and TM-HA/ELP composite scaffolds aimed at treating early degenerating NP tissue of the IVD. Both TM-HA and TM-HA/EP4 can be injected and subsequently cross-linked from their initial viscous form into stable hydrogels, *in situ* under physiologic conditions (37 C, pH 7.4) and *in vivo*, in a clinically reasonable time period (10–15 minutes). As DDD features both biologic and biomechanical derangement, it is essential to consider both these variables in biomaterial development. HA's large negative charge enables it to attract and retain water and makes it an interesting therapeutic candidate that has motivated its incorporation into NP scaffolds.^{4–8,18,19} Current commercially available HA formulations are viscous liquids, and there is a desire to enhance mechanical strength to lessen issues relating to the extravasation of injectable

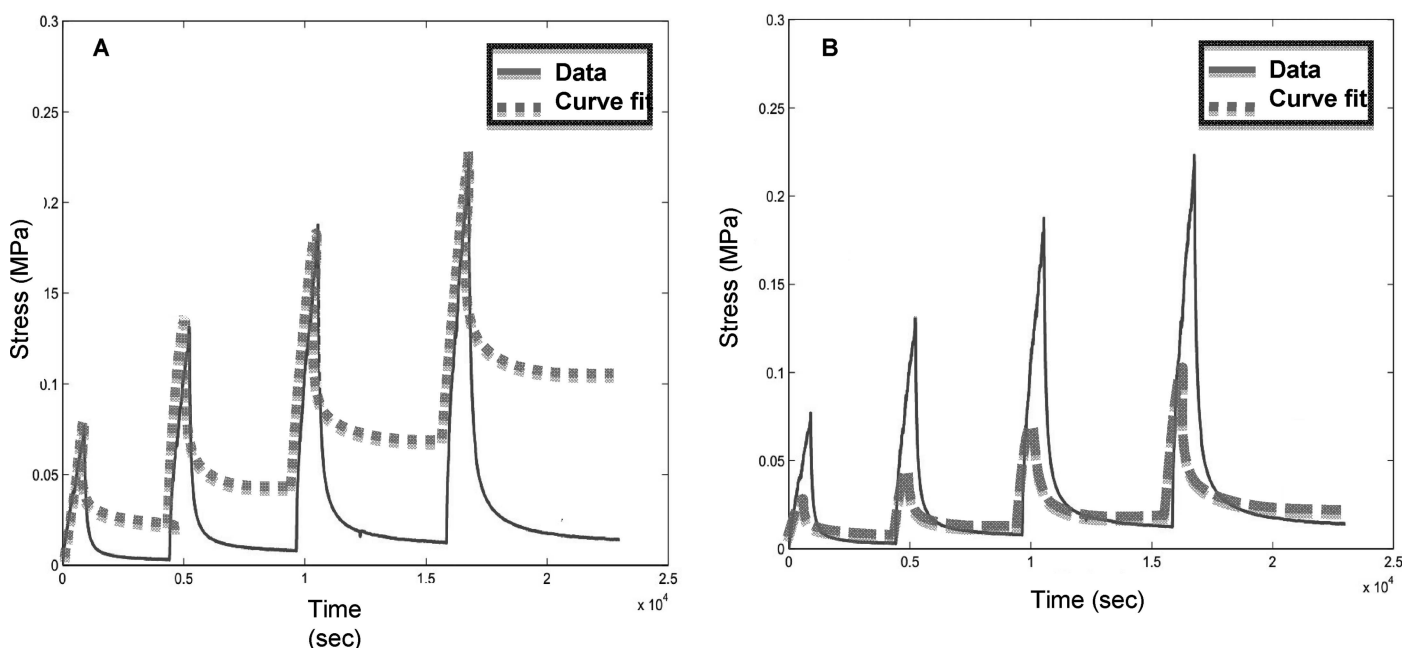


Figure 3. Attempted curve fitting of confined compression data to the permeability parameters of the nonlinear biphasic model of Holmes and Mow with parameters adjusted to fit peak stress (A) and equilibrium stress (B).

TABLE 3. Mean Peak Stress (\pm SD) for Each Hydrogel Formulation at Successive Strain Levels

	Mean Peak Stress (KPa)			
	10% Strain	20% Strain	30% Strain	40% Strain
HA	67.0 \pm 6.4	111.5 \pm 15.5	144.6 \pm 18.9*	160.5 \pm 15.9 [♦]
3:1	67.2 \pm 9.2	116.3 \pm 12.6	145.3 \pm 9.2§	176.1 \pm 16.3
2:1	69.6 \pm 12.7	118.2 \pm 10.8	154.2 \pm 8.2	170.0 \pm 16.5
1:1	78.9 \pm 19.7	130.0 \pm 19.2	171.6 \pm 11.7 *§	198.7 \pm 26.6 [♦]

*§,♦ matched statistically significant differences ($P < 0.05$).

materials either when applied therapeutically to the IVD or when the IVD experiences physiologic loads. TM-HA can be cross-linked into a hydrogel providing a more mechanically robust, three-dimensional environment that may be beneficial to supporting maintenance of NP cell phenotype.^{12,20} These hydrogels provide an environment similar to the charged, hydrated ECM of native human NP tissue. Incorporation of EP4, an injectable molecule that self-assembles into fibrils and demonstrates extensibility and recoil,¹⁰ as rebar in the scaffold construct was explored in this study with a goal toward further improving the mechanical strength and stiffness of TM-HA.

The *in vitro* experiments demonstrated that both the TM-HA and TM-HA/EP4 hydrogels examined maintained acceptable cell viability and phenotype for human IVD cells during the time periods evaluated. Although a reduction in overall viability from 78% to 70% was observed from 1 through 3 weeks in tissue culture, it is important to consider that the cells evaluated were from degenerate human surgical specimens under static culture conditions. The observed viability in our study is within the range reported for other NP scaffolds in the recent literature.^{21–24} These values are particularly relevant as the therapeutic target disc will similarly contain degenerate host tissue and NP cells.

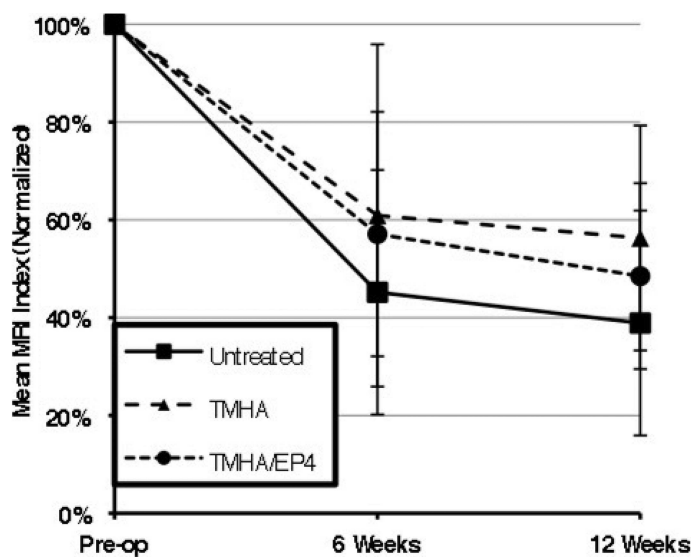


Figure 4. Mean MRI index for untreated and treated IVD, demonstrating a slower rate of decline in IVDs treated with TM-HA or TM-HA/EP4 hydrogels.

Two important qualitative observations can be made from the Live/Dead stained constructs. First, an even distribution of cells was found within both scaffold formulations demonstrating the effectiveness of scaffold preparation techniques used and the advantage of cross-linking the hydrogels around the cell after cell/scaffold mixing to optimize cell dispersion. Second, the spherical appearance of cells and presence of collagen type II within the scaffolds indicate that they form a supportive environment for maintenance of NP-like cell phenotype, conducive to expression of appropriate ECM molecules.

The feasibility of the surgical technique in discal delivery taking advantage of the ability of the hydrogels to cross-link *in vivo* within an acceptable time was demonstrated in the preclinical animal model. The *in vivo* MRI data, gross pathology, and histology data confirmed that there was no evidence of severe chronic inflammatory response to the implanted materials. As evidenced by the study MRI data on disc volume and signal intensity, hydrogels alone in the absence of cells or bioactive molecules are likely not potent enough of a stimulus to halt and/or reverse the process of IVD degeneration. Large standard deviations were noted in the MRI indexes reported, similar to those reported by Sobajima *et al*¹⁷ in the original description of this animal model. *Post hoc* power calculations based on the variance observed in this study with an α of 0.05 and β of 0.20 indicate that approximately 100 IVDs per group would be required to detect a 15% difference between the treatment and control groups at 12 weeks.

The addition of EP4 to TM-HA improved biomechanical properties but did not appear to positively or negatively impact IVD cell viability or activity when compared with TM-HA alone. The mean H_{A0} for the 2:1 TM-HA/EP4 hydrogel did not fall in between that of the 3:1 and 1:1 formulation, in contrast to what would have been expected. The standard deviation for the 2:1 formulation was also higher (± 6.2 KPa) than that of the other formulations (± 4.8 KPa for TMHA only, ± 3.3 KPa for 3:1, ± 4.8 KPa for 1:1). A possible explanation of this behavior anomaly may be variability in the production of the 2:1 hydrogel. This may also account for the difference in β when compared with the other formulations.

The discrepancy between the permeability parameters of the nonlinear biphasic model and the experimental data for the TM-HA and TM-HA/EP4 hydrogels observed in this study may be due to flow-independent intrinsic viscoelasticity

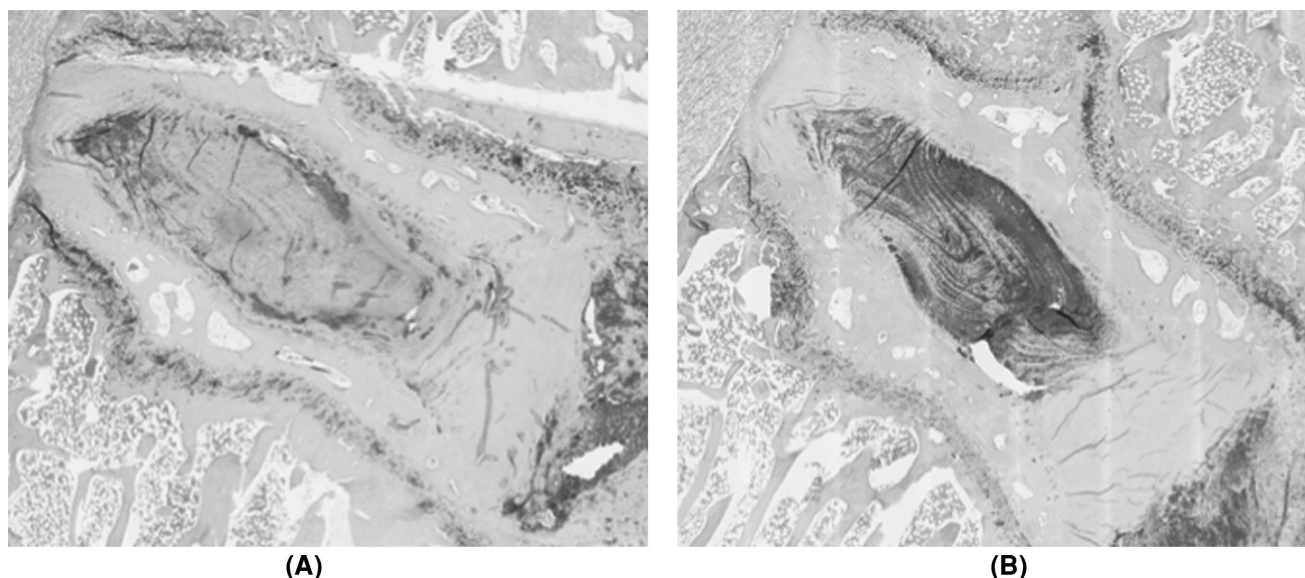


Figure 5. Alcian blue stained histologic sections of injured but untreated NZW rabbit IVD (A) and an IVD treated with the TM-HA hydrogel at 12 weeks. Deeper blue stain in the treated IVD suggests higher proteoglycan content (B).

of the matrix not accounted for in the model used. This is a phenomenon that has been observed in other tissues and biomaterials.^{25,26}

It is also important to note that the aggregate moduli of these formulations were still considerably less stiff than values reported for native mammalian NP tissue (310–1000 KPa).^{15,27} Although addition of greater numbers of EP4 to TM-HA results in a stiffer construct, a limiting consideration is that the addition of greater numbers of the largely hydrophobic EP4 may negate some of the beneficial effects of HA. An interesting positive observation of mechanical testing was that of time-dependent loading characteristics with high-peak stresses achieved during loading of the scaffolds. These results are within the range reported by Perie *et al*¹⁵ for bovine nucleus. Performance of TM-HA materials with EP4 under cyclic loading conditions merits further investigation.

CONCLUSION

TM-HA-based hydrogels provide a hospitable environment for human IVD cells and possess material characteristics, particularly when supplemented with ELPs that are attractive for potential application as an injectable NP supplement.

➤ Key Points

- ❑ Both biomechanical and biologic characteristics are important in selecting scaffolds for IVD tissue engineering.
- ❑ The addition of ELP to TM-HA-based hydrogels resulted in a stiffer construct, which is less stiff than native NP but has time-dependant loading characteristics that may be desirable when injected into the IVD.

- ❑ Human IVD cells maintained viability and apparent phenotype when cultured in TM-HA-based hydrogels for 3 weeks.
- ❑ The TM-HA-based materials were found to have appropriate material characteristics and biocompatibility when tested in a small animal model of disc degeneration.

Acknowledgments

Authors thank Deborah Denis and Aimee Gallant for their help with patient recruitment, Dr. Margarete Aikens for her assistance with the preclinical model of disc degeneration, and Dr. Warren Foltz for his help with the MRI.

Ethics approval for this work was obtained from the Sunnybrook Health Sciences Centre Research Ethics Board and Animal Care Committee.

References

1. Roughley PJ. Biology of intervertebral disc aging and degeneration: involvement of the extracellular matrix. *Spine* 2004; 29:2691–9.
2. Stern S, Lindenhayn K, Schultz O, et al. Cultivation of porcine cells from the nucleus pulposus in a fibrin/hyaluronic acid matrix. *Acta Orthop Scand* 2000;71:496–502.
3. Pfeiffer M, Boudriot U, Pfeiffer D, et al. Intradiscal application of hyaluronic acid in the non-human primate lumbar spine: radiological results. *Eur Spine J* 2003;12:76–83.
4. Halloran DO, Grad S, Stoddart M, et al. An injectable cross-linked scaffold for nucleus pulposus regeneration. *Biomaterials* 2008;29:438–47.
5. Revell PA, Damien E, Di Silvio L, et al. Tissue engineered intervertebral disc repair in the pig using injectable polymers. *J Mater Sci Mater Med* 2007;18:303–8.
6. Yang G, Woodhouse KA, Yip CM. Substrate-facilitated assembly of elastin-like peptides: studies by variable-temperature in situ atomic force microscopy. *J Am Chem Soc* 2002;124:10648–9.
7. Yang SH, Chen PQ, Chen YF, et al. An in-vitro study on regeneration of human nucleus pulposus by using gelatin/chondroitin-6-

- sulfate/hyaluronan tri-copolymer scaffold. *Artif Organs* 2005;29:806–14.
8. Yang SH, Chen PQ, Chen YF, et al. Gelatin/chondroitin-6-sulfate copolymer scaffold for culturing human nucleus pulposus cells *in vitro* with production of extracellular matrix. *J Biomed Mater Res B Appl Biomater* 2005;74:488–94.
 9. Shu XZ, Liu Y, Palumbo F, et al. Disulfide-crosslinked hyaluronan-gelatin hydrogel films: a covalent mimic of the extracellular matrix for *in vitro* cell growth. *Biomaterials* 2003;24:3825–34.
 10. Bellingham CM, Lillie MA, Gosline JM, et al. Recombinant human elastin polypeptides self-assemble into biomaterials with elastin-like properties. *Biopolymers* 2003;70:445–55.
 11. Bellingham CM, Woodhouse KA, Robson P, et al. Self-aggregation characteristics of recombinantly expressed human elastin polypeptides. *Biochim Biophys Acta* 2001;1550:6–19.
 12. Chiba K, Andersson GB, Masuda K, et al. Metabolism of the extracellular matrix formed by intervertebral disc cells cultured in alginate. *Spine* 1997;22:2885–93.
 13. Gruber HE, Stasky AA, Hanley EN, Jr. Characterization and phenotypic stability of human disc cells *in vitro*. *Matrix Biol* 1997;16:285–8.
 14. Holmes MH, Mow VC. The nonlinear characteristics of soft gels and hydrated connective tissues in ultrafiltration. *J Biomech* 1990;23:1145–56.
 15. Perie D, Korda D, Iatridis JC. Confined compression experiments on bovine nucleus pulposus and annulus fibrosus: sensitivity of the experiment in the determination of compressive modulus and hydraulic permeability. *J Biomech* 2005;38:2164–71.
 16. Masuda K, Aota Y, Muehleman C, et al. A novel rabbit model of mild, reproducible disc degeneration by an annulus needle puncture: correlation between the degree of disc injury and radiological and histological appearances of disc degeneration. *Spine* 2005;30:5–14.
 17. Sobajima S, Kompel JF, Kim JS, et al. A slowly progressive and reproducible animal model of intervertebral disc degeneration characterized by MRI, X-ray, and histology. *Spine* 2005;30:15–24.
 18. Ghosh P, Guidolin D. Potential mechanism of action of intra-articular hyaluronan therapy in osteoarthritis: are the effects molecular weight dependent? *Semin Arthritis Rheum* 2002;32:10–37.
 19. Alini M, Roughley PJ, Antoniou J, et al. A biological approach to treating disc degeneration: not for today, but maybe for tomorrow. *Eur Spine J* 2002;11(Suppl 2):S215–20.
 20. Gruber HE, Hanley EN, Jr. Human disc cells in monolayer *vs.* 3D culture: cell shape, division and matrix formation. *BMC Musculoskelet Disord* 2000;1:1.
 21. Richardson SM, Hughes N, Hunt JA, et al. Human mesenchymal stem cell differentiation to NP-like cells in chitosan-glycerophosphate hydrogels. *Biomaterials* 2008;29:85–93.
 22. Roughley P, Hoemann C, DesRosiers E, et al. The potential of chitosan-based gels containing intervertebral disc cells for nucleus pulposus supplementation. *Biomaterials* 2006;27:388–96.
 23. Mwale F, Iordanova M, Demers CN, et al. Biological evaluation of chitosan salts cross-linked to genipin as a cell scaffold for disk tissue engineering. *Tissue Eng* 2005;11:130–40.
 24. Reza AT, Nicoll SB. Characterization of novel photocrosslinked carboxymethylcellulose hydrogels for encapsulation of nucleus pulposus cells. *Acta Biomater* 2010;6:179–86.
 25. Huang CY, Mow VC, Ateshian GA. The role of flow-independent viscoelasticity in the biphasic tensile and compressive responses of articular cartilage. *J Biomech Eng* 2001;123:410–7.
 26. Mak AF. The apparent viscoelastic behavior of articular cartilage—the contributions from the intrinsic matrix viscoelasticity and interstitial fluid flows. *J Biomech Eng* 1986;108:123–30.
 27. Johannessen W, Elliott DM. Effects of degeneration on the biphasic material properties of human nucleus pulposus in confined compression. *Spine* 2005;30:E724–9.